Approximate solutions for an acoustic plane wave propagation in a layer with high sound speed gradient

Alex Zinoviev and Adrian D. Jones

Maritime Division, Defence Science and Technology Organisation, Edinburgh, 5111, Australia

ABSTRACT

The present authors previously obtained an exact solution for propagation of the incident acoustic plane wave in a wind-induced bubbly surface layer where sound speed gradient is high. Based on the solution, the dependence of the grazing angle of the energy flux vector of the incident wave at the surface on the grazing angle of the incident wave at the bottom of the layer was obtained and utilised for calculations of the surface reflection loss. However, the solution in its original formulation is represented via an infinite slowly converging series which makes the use of the solution in practical calculations difficult. In this paper, this solution is simplified with the assumption that the grazing angle at the bottom of the layer as well as some other parameters depending on the frequency and wind speed are small. The convergence of the infinite series is improved using a special technique. Approximate solutions are obtained for the cases where the small parameters can be neglected and where the terms up to the third order with respect to the small parameters are taken into account. Zones of validity are derived for the approximate solutions as well as for the Snell's law of ray acoustics. The results of this paper allow the prediction of the grazing angle at the surface within the zones of validity of the approximate solutions using simple calculations with only the wind speed, the frequency and the equilibrium sound speed as the input parameters.

INTRODUCTION

Trapping acoustic energy within a medium, due to a favourable sound speed gradient, is a well-known effect. An example of duct trapping occurs within an isothermal surface layer in an ocean for which the sound speed increases with depth due to the increasing hydrostatic pressure. Formation of such a duct may lead to a significant increase in the propagation range, as is well known.

At the same time, the propagation of sound wave in the layer is significantly complicated by the roughness of the ocean surface. Due to the roughness, the acoustic energy can be scattered in non-specular directions thus considerably increasing the reflection loss and correspondingly decreasing the propagation range. As a result, the roughness of the ocean surface must be taken into consideration in any realistic model of sound propagation within the surface duct.

Existing models of sound scattering at the rough ocean surface usually take the grazing angle at the surface as an input parameter. In some instances the grazing angle at the surface can be calculated by means of Snell's law of ray acoustics. However, in situations where the sound speed change in the surface duct is considerable on the scale of the acoustic wavelength, Snell's law may no longer be applied for calculating the grazing angle and a wave-based theory becomes necessary for this purpose. For example, such a situation can be caused by the presence of air bubbles in the ocean near the surface. These wind-induced bubbles change the compressibility of water thus leading to significant reduction of the sound speed near the surface.

Jones et al. (2011) suggested a model for evaluating the loss of acoustic energy due to reflection from the rough ocean surface. The model was called "JBZ" by the authors and is based on the Hall-Novarini bubble population model (Hall, 1989, Keiffer et al., 1995) as well as on the calculations of the sound speed in the bubbly layer by Ainslie (2005). An integral part of the JBZ model is also a novel method of evaluating the grazing angle at the surface. The method is founded on a wave-based solution of the wave equation in a vertically stratified layer. The solution is based on a formulation provided by Brekhovskikh (1960) for a transitional layer between two media with different values of the equilibrium sound speed. This solution has been considered in detail by Zinoviev et al (2012). It has been demonstrated that, if the incident grazing angle at the bottom of the bubbly layer is of the order of a few degrees or less, the grazing angle at the surface may differ significantly from the value predicted by Snell's law.

The lesser of two values for the grazing angle at the surface, one of which was predicted by Snell's law and the other one by the wave-based solution, has been utilised in calculations of the transmission loss using the JBZ model (Jones et al., 2011). The results of the calculations have shown good correlation with the results obtained using a Parabolic Equation transmission code.

Although the JBZ model showed its validity, in the original formulation the solution for the grazing angle at the surface contains a slowly converging infinite series and depends on parameters of the layer which need to be obtained from matching the sound speed profile in the real layer and the transitional layer described by Brekhovskikh (1960). Therefore, to make the wave-based method of calculating the grazing angle at the surface more practicable, its theoretical formulation needs to be simplified.

This paper is devoted to finding and justifying simplified approximate solutions for the grazing angle at the surface. In the first section, the exact solution obtained by Zinoviev et al. (2012) is reviewed. In the second section, major steps in the derivation of the approximate simplified solutions are demonstrated. The third section contains justification of zones of validity of the obtained approximate solutions and of the Snell's law. Finally, in the fourth section, examples of the dependencies of the grazing angle at the surface on the incident grazing angle for different frequencies and wind speeds are shown and discussed**.**

EXACT SOLUTION FOR SOUND PROPAGATION IN THE SURFACE LAYER

Sound speed profile in the surface layer

Zinoviev et al. (2012) showed that the sound speed profile based on the Ainslie's calculations of sound speed in the mixture of water and bubbles can be well approximated by sound speed profile in the transitional layer considered by Brekhovskikh (1960). This derivation is reviewed below.

Assume that the vertical coordinate, *z*, is directed from the surface. If the sound speed far below the surface layer is c_0, the profile of the transitional layer can be determined by the following equation:

$$c(z) = c_0\sqrt{\frac{1-N}{1-N\dfrac{e^{mz}}{1+e^{mz}}}}, \quad z > 0. \tag{1}$$

In Equation (1), *N* and *m* are parameters of the layer. *N* characterises the "strength" of the layer and is determined by the following equation:

$$N = 1-\left(\frac{2c_s - c_0}{c_0}\right)^2, \tag{2}$$

where c_s is the sound speed at the surface. As $m = 0$ corresponds to an infinitely wide layer, whereas at $m \to \infty$ the layer is infinitely thin, it can be said that $1/m$ describes the "thickness" of the layer.

It is convenient to assume that the surface of water in the Ainslie's layer does not coincide exactly with the surface $z = 0$ in the transitional layer, but, instead, it is located at some positive depth $z = z_0$. In this case, the following equation provides the link between the parameters *m* and z_0:

$$m\left[z+z_0\right] = \ln\left\{\frac{\dfrac{c^2(z)}{c_0^2\left[1-N\right]}-1}{1-\dfrac{c^2(z)}{c_0^2}}\right\}. \tag{3}$$

To determine *m* and z_0, it is necessary to consider Equation (3) together with another equation chosen to make sure that the transitional layer profile represents the "best fit curve" for the Ainslie's profile. This procedure is explained in detail by Zinoviev et al. (2012).

Solution for the grazing angle at the surface

Brekhovskikh (1960) showed that, if a plane wave with the wave vector, $\mathbf{k_0}$, approaches the transitional layer from below with the grazing angle, θ_0, between the wave vector and the horizontal axis, *x*, the solution for the acoustic pressure within the layer can be written with the use of hypergeometric series. By applying Brekhovskikh's solution for the acoustic pressure to the transitional layer Zinoviev et al. (2012) derived a system of equations for the grazing angle, θ_s, of the energy density vector, $\mathbf{q}$, at the surface. The vector $\mathbf{q}$ is determined via the acoustic pressure, *p*, and the particle velocity, $\mathbf{v}$, as $\mathbf{q} = p\mathbf{v}$. After some parameter substitutions the system of equations for finding θ_s takes the following form:

$$\theta_s = \tan^{-1}\left(\frac{\mathrm{Re}\left(pv_n^*\right)}{\mathrm{Re}\left(pv_x^*\right)}\right), \tag{4}$$

$$p(x,z) = Z(z)e^{ik_0 x\sin\theta_0}, \tag{5}$$

$$Z(z) = (1-\xi)G(\xi), \tag{6}$$

$$\xi = -e^{mz}, \tag{7}$$

$$v_x = \frac{k_0\sin\theta_0}{\omega\rho}p, \tag{8}$$

$$v_n = \frac{i}{\omega\rho}\frac{\partial p}{\partial z}, \tag{9}$$

$$G(\xi) = \sum_{n=0}^{\infty} g_n(\xi), \tag{10}$$

$$g_0(\xi) = \xi^{-(1+i\delta)}, \tag{11}$$

$$g_{n+1}(\xi) = \frac{g_n(\xi)}{\xi}\left(1+\frac{\mu^2}{(n+1)(n+2i\delta+1)}\right), \tag{12}$$

$$\delta = \frac{k_0}{m}\sin\theta_0\sqrt{1-N}, \tag{13}$$

$$\mu = \frac{k_0}{m}\sqrt{N} = \frac{2\pi f}{mc_0}\sqrt{N}. \tag{14}$$

In Equations (4) to (14), as well as in the analysis below, *p* is the acoustic pressure, v_n and v_x are vertical and horizontal components of the particle velocity, $\omega = 2\pi f$ is the cyclic frequency of the acoustic wave (temporal dependence $e^{-i\omega t}$ is assumed), ρ is the equilibrium water density, $G(\xi)$ is an infinite series originating from the hypergeometric series, and δ and μ are auxiliary variables. The equilibrium sound speed far below the layer, c_0, is assumed to be 1500 m/s. Equations (4) to (14) represent the *exact* solution for a plane wave propagation in the transitional layer as no assumptions have been made about values of any of the parameters.

DERIVATION OF APPROXIMATE SOLUTIONS FOR THE GRAZING ANGLE AT THE SURFACE

Small parameters for approximations

It is difficult to use Equations (4) to (14) in practical calculations for two reasons. First, they include an infinite series, $G(\xi)$, which is converging slowly near the ocean surface, where $|\xi| \to 1$. Second, to find the layer parameters *m*, *N* and z_0, it is necessary to know the real sound speed profile in the bubbly layer, which is not always feasible.

However, it is possible to simplify the solution for θ_s by making assumptions that some parameters are small and subsequently using Taylor series to neglect terms of higher orders with respect to these parameters. First of all, it is known that, during the sound propagation in the surface duct, the incident angles are normally not larger than a few degrees. Therefore, it is reasonable to assume that the incident grazing angle at the bottom of the bubbly layer, θ_0, is small:

$$\theta_0 \le 3° \approx 0.052 \text{ rad} << 1. \tag{15}$$

Also, some parameters of the bubbly layer in realistic conditions can be considered to be small. Table 1 shows the parameters of the layer calculated for four values of the wind speed using the method described by Zinoviev et al. (2012). The wind speed in the present analysis refers to the height of 19.5 m above the ocean surface.

Table 1. Dependence of the calculated parameters of the layer on the wind speed.

Wind speed, m/s	5	7.5	10	12.5
N	0.0043	0.014	0.034	0.064
m, m^{-1}	3.1	3.1	2.1	1.5
z_0, m	0.0010	0.0035	0.012	0.034

It is clearly seen from Table 1 that, at the wind speeds of interest, the following assumptions can be made:

$$N < 0.1 << 1, \tag{16}$$

$$mz_0 < 0.1 << 1. \tag{17}$$

Taking into consideration Equations (15) to (17), all terms in a Taylor series containing θ_0, N and mz_0 of the second and higher orders are neglected in this analysis.

At the same time, the parameters δ and μ determined by Equations (13) and (14) contain the small parameters multiplied by the ratio k_0/m, which is proportional to the frequency and may be significantly larger than unity at frequencies of a few kilohertz. Therefore, terms of higher orders than the first one with respect to δ and μ are required to be taken into account. In this analysis, the terms containing δ and μ of the orders up to the third one are used and the terms of higher orders are neglected.

Improving convergence of the infinite series

Detailed description of the calculations leading to the approximate solutions is considered to be outside the scope of this work. However, these calculations involve an important step – an application of a special technique to significantly improve the convergence of the infinite series. This step is described in this section.

It is clear that the infinite series $G(\xi)$ described by Equations (10) to (12) converges at all depths $z > 0$. Indeed, the term in the brackets in Equation (12) tends to unity if $n \to \infty$. Also, the following condition is satisfied for the variable ξ:

$$\left|\xi\right|_{z>0} = e^{mz}\Big|_{z>0} > 1. \tag{18}$$

However, close to the surface, where $z \to z_0$, the convergence is slow due to the small value of the exponent mz. Numerical experiments show that, for the series $G(\xi)$ to converge, a large number of terms need to be taken into account. Obviously, derivation of a simplified approximate solution requires this slow convergence to be improved.

Such improvement is carried out here using Kummer's transformation (Linton, 1998). After expanding into Taylor series over small parameters the term in the brackets in Equation (12) can be written as follows:

$$1+\frac{\mu^2}{(n+1)(n+2i\delta+1)} \approx 1+\frac{\mu^2}{(n+1)^2} - 2i\mu^2\frac{\delta}{(n+1)^3}. \tag{19}$$

Now the infinite series $G(\xi)$ takes the form of

$$G(\xi) \approx \xi^{-i\delta-1}\left(1+\frac{a_1}{\xi}+\frac{a_2}{\xi^2}+...\right), \tag{20}$$

where

$$a_n = \prod_{j=1}^{n}\left(1+\frac{\mu^2}{j^2}-2i\frac{\delta\mu^2}{j^3}\right). \tag{21}$$

According to Kummer's transformation, the sum of an infinite converging series, x_n, can be represented by the following equation:

$$\sum_{n=1}^{\infty} x_n = \sum_{n=1}^{\infty}\left(x_n - x_n\big|_{n\to\infty}\right) + S, \tag{22}$$

where

$$S = \sum_{n=1}^{\infty} x_n\big|_{n\to\infty}. \tag{23}$$

Assume the sum S in Equation (23) can be found analytically. The infinite series in the right-hand part of that equation converges much faster than the series in the left-hand part, as the two terms in the brackets asymptotically tend to each other and their difference tends to zero with increasing n.

For the series $G(\xi)$ under consideration, it can be found numerically that the coefficients a_n at large n tend to the following expression:

$$a_n\big|_{n\to\infty} = 1 + b\mu^2 - ai\mu^2\delta, \tag{24}$$

where a and b are constants determined as

$$a \approx 2.404, \quad b \approx 1.645. \tag{25}$$

Applying Kummer's transformation to the series $G(\xi)$ allows one to re-write the series in the following form:

$$G(\xi) \approx \xi^{-i\delta-1}\left(1+\frac{1+b\mu^2-ai\mu^2\delta}{\xi-1} + \sum_{n=1}^{\infty}\frac{a_n-\left(1+b\mu^2-ai\mu^2\delta\right)}{\xi^n}\right). \tag{26}$$

It can be shown by numerical calculations that the series determined by Equation (26) converges quickly.

Approximate solutions for the grazing angle at the surface

An investigation of the series in Equation (26) shows that only a few terms in the series are needed to obtain a solution with a good degree of approximation. As successive terms of the series have opposite signs, the total sum of the series is always between two successive partial sums.

In this analysis, the approximate solutions have been obtained for one and two terms in the series. The substitution of

Equation (26) into Equations (4) to (14), expanding the resulting equations into the Taylor series where necessary and neglecting terms of higher orders leads to the following simple equations for the grazing angle at the surface for one and two terms in the series respectively:

$$\theta_s^{(1)} \approx \theta_0\left(1+1.19\mu^2\right), \tag{27}$$

$$\theta_s^{(2)} \approx \theta_0\left(1+1.96\mu^2\right), \tag{28}$$

where

$$\mu = \frac{2\pi f}{mc_0}\sqrt{N}. \tag{29}$$

Note that the parameter μ can be considered as non-dimensional frequency. Due to the opposite signs of successive terms of the infinite series, the full solution for θ_s should be found between $\theta_s^{(1)}$ and $\theta_s^{(2)}$. The validity of Equations (27) and (28) is discussed further in this analysis.

Determining the layer parameters by polynomial curve fitting

The obtained approximate solutions (Equations (27) and (28)) include the layer parameters N and m. Note that the parameter z_0 is absent from these solutions. As shown above, the layer parameters can be found by matching the sound speed profile of the bubbly layer to the sound speed profile of the transitional layer. It is clear, however, that this method is not useful for practical purposes.

It is demonstrated below that the parameters N and m can be also found by polynomial curve fitting using only the wind speed, W, as an input parameter. Figures 1 and 2 show values for N and m calculated using the sound speed matching algorithm as described in Zinoviev et al (2012) as well as by means of the curve fitting (best fit curve) method. The equations determining the best fit curves are as follows:

$$\begin{aligned} N = {} & 2.70\times10^{-5}W^3 + 1.18\times10^{-4}W^2 \\ & -6.40\times10^{-4}W + 1.11\times10^{-3}, \end{aligned} \tag{30}$$

$$m = \begin{cases} 3.10 & \text{if} \quad W \le 8 \\ -1.01\times10^{-2}W^3 + 3.67W^2 \\ -4.66W + 22.0 & \text{if} \quad W > 8 \end{cases} \tag{31}$$

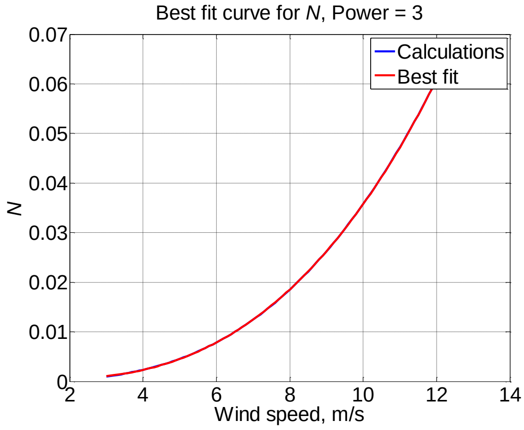

Figure 1. Parameter N calculated by means of the sound speed matching algorithm in comparison with the best fit curve.

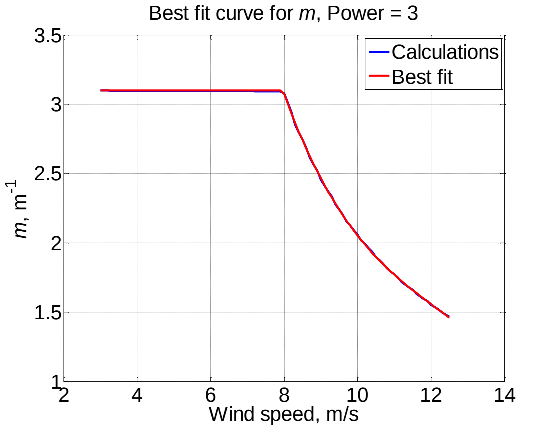

Figure 2. Parameter m calculated by means of the sound speed matching algorithm in comparison with the best fit curve.

It is clear from Figures 1 and 2 that polynomial curve fitting of the third power approximates the dependencies of the parameters N and m on the wind speed within the given range to such an extent that the original curves and the best fitted ones are virtually indistinguishable. Note that m is constant below the wind speed of 8 m/s due to a peculiarity in the Hall-Novarini bubble population model.

Numerical calculations show that, within the range of realistic values of c_0, m does not depend on the equilibrium sound speed, c_0, and N depends on c_0 only slightly. Therefore, Equations (30) and (31) provide a tool for determining the parameters of the transitional layer acoustically equivalent to the bubbly surface layer with only the wind speed as an input parameter.

AREAS OF VALIDITY OF THE SOLUTIONS FOR THE GRAZING ANGLE AT THE SURFACE

Equations (27) and (28) show that, if μ^2 is small enough, the grazing angles at the ocean surface, θ_s, and at the bottom of the surface layer, θ_0, can be considered equal and, consequently, the refraction in the layer can be neglected. Assume that the parameter μ^2 can be considered to be small for this purpose if the following condition is satisfied:

$$\mu^2 < 0.1. \tag{32}$$

Taking into consideration Equation (29), the criterion of the absence of refraction in the layer can be written as

$$f < 0.0503\frac{mc_0}{\sqrt{N}}, \tag{33}$$

where N and m are determined via the wind speed, W, by Equations (30) and (31).

Figure 3 shows the areas of validity of the approximate solutions on the frequency/wind speed plane. The case of no refraction corresponds to the lowest (green) curve, so that refraction can be neglected at any point below this curve.

it is reasonable to assume that the next term in Equations (27) and (28) with respect to the parameter μ will be of the order of μ^4 and, therefore, the condition of validity of Equations (27) and (28) can be written as

$$\mu^4 < 0.1, \tag{34}$$

which leads to the following condition for the corresponding frequency range:

$$f < 0.0900\frac{mc_0}{\sqrt{N}}. \tag{35}$$

In Figure 3, the area of validity of Equations (27) and (28) is below the cyan line. It can be seen that these approximate solutions are valid at higher frequencies and wind speeds than the solution which neglects the influence of bubbles on refraction altogether.

Equations (33) and (35) together with Equations (30) and (31) represent a simple method of determining the frequency ranges where the refraction in the bubbly layer can be neglected altogether and where the approximate solutions are valid. The input parameters are the wind speed, which can be easily measured, and the equilibrium sound speed, which, in real conditions, is close to a constant value of 1500 m/s.

The well-known Snell's law of ray acoustics, in application to the layer under consideration, can be formulated as

$$\frac{\cos\theta_s}{\cos\theta_0} = \frac{c_s}{c_0}. \tag{36}$$

As $c_s < c_0$ for the surface bubbly layer, Equation (36) shows that the grazing angle θ_s at the surface is not zero even if the incident grazing angle θ_0 approaches zero. This directly contradicts Equations (27) and (28), which show that $\theta_s \to 0$ if $\theta_0 \to 0$. To resolve this contradiction, it is necessary to determine the area of applicability of the Snell's law in the bubbly layer.

As shown above, Equations (27) and (28) have been obtained using the assumptions that some parameters are small and subsequently considering only low-order terms with respect to these parameters. It is clear, however, that taking into consideration terms of higher orders in Equations (27) and (28) will not lead to the Snell's law, as the higher order terms will also vanish at $\theta_0 \to 0$. Therefore, it can be concluded that the parameters assumed small in the analysis leading to Equations (27) and (28) are not small when Snell's law is valid.

Numerical calculations show that the full solution for the grazing angle at the surface tends to the predictions of the Snell's law with increasing θ_0 (Zinoviev et al., 2012). Out of the small parameters described earlier in this paper only one parameter, δ, which is determined by Equation (13), depends on θ_0. Therefore, it is reasonable to assume that the Snell's law is valid if δ is large enough for the Taylor series over this parameter *not* to be valid. Assume that the following condition for δ is satisfied in this case:

$$\delta > 0.5. \tag{37}$$

Considering that N is small, Equation (37) can be used to derive the following condition on frequency to determine the validity of the Snell's law in the application to the surface bubbly layer:

$$f > 0.0796\frac{mc_0}{\theta_0}. \tag{38}$$

In Figure 3, the areas of validity of the Snell's law are shown for the incident angle θ_0 of 1.5 and 3 degrees. The Snell's law is valid at any point *above* the corresponding curves.

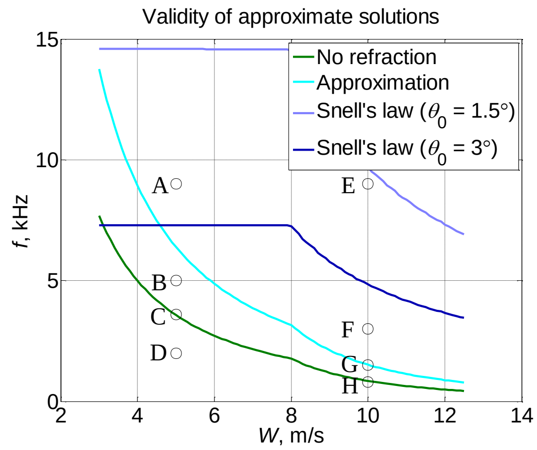

Figure 3. Areas of validity of approximate solutions. The solutions corresponding to the case of no refraction and to the approximation with respect to the small parameters are valid *below* the respective curves. The Snell's law is valid *above* the respective curves. Circles denote the points for which graphs are shown in Figure 4.

It can be seen from Figure 3 that the refraction in the layer can be neglected if the wind speed and/or the frequency are not too high. In this case the acoustic wavelength is large in comparison to the depth of the layer, so that the layer cannot affect significantly the acoustic wave propagation. It is also clear that the obtained approximate solutions (Equations (27) and (28)) are valid at larger intervals of the wind speed and frequency according to the assumption that the non-dimensional frequency μ is small but non-zero.

Equation (38) demonstrates that the area of validity for the Snell's law depends on the incident grazing angle θ_0. The lowest frequency where the Snell's law is valid is inversely proportional to θ_0. This leads to an important conclusion that, for each frequency, there is a critical incident grazing angle such that the Snell's law is not valid at any angle smaller than this critical value.

In general, the approximate solutions derived and investigated in this paper can be used if the corresponding point on the wind speed/frequency plane is below the green line in Figure 3. If the incident angle is larger than the angle determined for a given frequency by Equation (38) Snell's law can be used to determine the grazing angle at the surface. In other cases the full solution needs to be used for this purpose.

DEPENDENCE OF THE GRAZING ANGLE AT THE SURFACE ON THE INCIDENT GRAZING ANGLE

In Figure 4, dependencies of the grazing angle at the surface, θ_s, on the incident grazing angle, θ_0, are shown for the combinations of values of the wind speed and frequency marked by circles in Figure 3. The letters near the circles in Figure 3 point to the corresponding graphs in Figure 4.

Figure 4D corresponds to the point in Figure 3 below the green line. It is clear that, in this case, the full solution and the solution for the case of no refraction are very close, which means that, as expected, the influence of bubbles on sound propagation can be neglected at this wind speed and frequency combination.

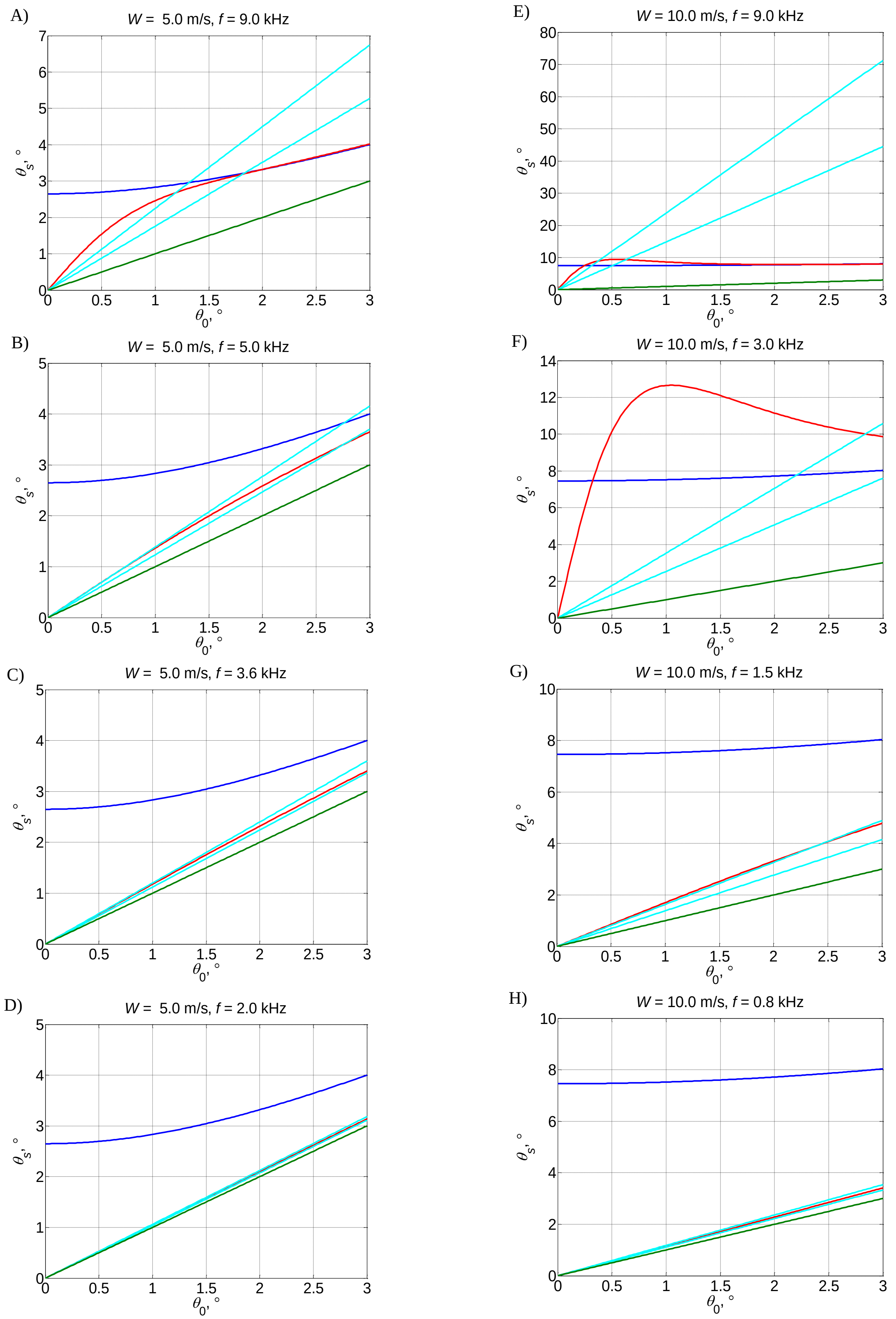

Figure 4. Dependence of the grazing angle at the surface on the incident grazing angle below the surface layer. Red line – full solution, top and bottom cyan lines – approximate solutions with two and one terms in the series respectively, green line – no refraction, blue line – Snell's law. The letter notations correspond to the points in Figure 3.

The points C and H in Figure 3 lie on the boundary of the area of validity of the no refraction case. It can be seen in the corresponding graphs in Figure 4 that the green line for the no refraction case is slightly below the red line for the full solution. At the same time, it can be seen that the approximate solutions are valid, as the red line lies between the two green straight lines for the approximate solutions. The same is applied also to Figure 4B.

The point G in Figure 3 is on the boundary of the area of validity of the approximate solutions. In the corresponding Figure 4G, the curve for the full solution lies very close to the line for the approximate solution with two terms in the series (the top green line).

The point F in Figure 3 lies in the area where the approximate solution is not valid. This is clearly seen in the corresponding Figure 4F. The maximum of the full solution curve is caused by the proximity of the frequency to one of the resonances described by Zinoviev et al. (2012).

The point A in Figure 3 is located above the line which marks the area of validity of the Snell's law at θ_0 = 3º. The corresponding figure 4A shows that, indeed, the full solution coincides with the Snell's law at θ_0 > 2º. Similar coincidence between the full solution and the Snell's law can be observed in Figure 4E at θ_0 > 1.5º.

Overall, the graphs depicted in Figure 4 confirm the criteria of validity determined by Equations (33), (35) and (38).

CONCLUSIONS

In this paper, an exact solution for plane wave propagation in a bubbly surface layer is simplified using assumptions that some parameters characterising the layer are small. An infinite series present in the equation for the acoustic pressure in the layer is transformed using Kummer's technique to improve its convergence. Approximate solutions are obtained for one and two terms in the series. It is shown that the full solution lies between the two approximate solutions if the underlying assumptions are valid.

Areas of validity with respect to the frequency, the wind speed, the sound speed, and the incident grazing angle are obtained for the approximate solutions as well as for the Snell's law. A criterion of validity is also obtained for the case where no significant refraction occurs in the layer.

It is shown that the parameters characterising the layer can be obtained by means of polynomial curve fitting of the third order with only the wind speed as an input parameter.

Dependencies of the grazing angle at the surface on the incident grazing angle at the bottom of the layer are calculated for several values of the wind speed and frequency. The obtained dependencies confirm the criteria of validity for the obtained approximate solutions.

Overall, the results of this paper demonstrate that, when a bubbly layer with high sound speed gradient is present near the ocean surface, the grazing angle at the surface can be predicted by means of a few simple equations, if the parameters of propagation satisfy the obtained criteria.

REFERENCES

Ainslie, MA 2005, 'Effect of wind-generated bubbles on fixed range acoustic attenuation in shallow water at 1–4 kHz', *J. of Acoust. Soc. Amer.*, vol. 118, no. 6, pp. 3513-23.

Jones, AD, Duncan, AJ, Bartel, DW, Zinoviev, A & Maggi, A 2011, 'Recent Developments in Modelling Acoustic Reflection Loss at the Rough Ocean Surface', *Proceedings of the Acoustics 2011*, Gold Coast, Australia.

Brekhovskikh, LM 1960, *Waves in layered media*, Academic Press, New York.

Hall, MV 1989, 'A comprehensive model of wind-generated bubbles in the ocean and predictions of the effects on sound propagation at frequencies up to 40 kHz', *J. of Acoust. Soc. Amer.*, vol. 86, no. 3, pp. 1103-17.

Keiffer, RS, Novarini, JC & Norton, GV 1995, 'The impact of the background bubble layer on reverberation-derived scattering strengths in the low to moderate frequency range', *J. of Acoust. Soc. Amer.*, vol. 97, no. 1, pp. 227-34.

Linton, CM 1998, 'The Green's function for the two-dimensional Helmholtz equation in periodic domain', *J. Eng. Math.*, vol. 33, pp. 377-402.

Zinoviev, A, Bartel, DW & Jones, AD 2012, 'An Investigation of Plane Wave Propagation through a Layer with High Sound Speed Gradient', *Proceedings of the ACOUSTICS 2012*, Fremantle, Australia.